Journal Pre-proof

Selection and characterization of non-ideal ionic liquids mixtures to be used in CO$_2$ capture

Mónia A.R. Martins, Gyanendra Sharma, Simão P. Pinho, Ramesh L. Gardas, João A.P. Coutinho, Pedro J. Carvalho

Please cite this article as: Mó.A.R. Martins, G. Sharma, Simã.P. Pinho, R.L. Gardas, Joã.A.P. Coutinho, P.J. Carvalho, Selection and characterization of non-ideal ionic liquids mixtures to be used in CO$_2$ capture, *Fluid Phase Equilibria* (2020), doi: https://doi.org/10.1016/j.fluid.2020.112621.

This is a PDF file of an article that has undergone enhancements after acceptance, such as the addition of a cover page and metadata, and formatting for readability, but it is not yet the definitive version of record. This version will undergo additional copyediting, typesetting and review before it is published in its final form, but we are providing this version to give early visibility of the article. Please note that, during the production process, errors may be discovered which could affect the content, and all legal disclaimers that apply to the journal pertain.
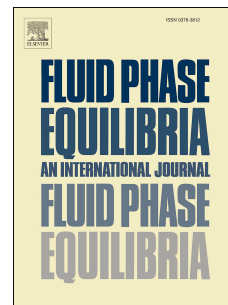
1

Selection and Characterization of non-ideal Ionic Liquids Mixtures to be used in CO$_2$ Capture

Mónia A. R. Martins,[1-3] Gyanendra Sharma,[4] Simão P. Pinho,[2,3] Ramesh L. Gardas,[4] João A. P. Coutinho[1] and Pedro J. Carvalho,[1*]

[1]CICECO – Aveiro Institute of Materials, Department of Chemistry, University of Aveiro, 3810-193 Aveiro, Portugal

[2]Associate Laboratory LSRE-LCM, Department of Chemical and Biological Technology, Polytechnic Institute of Bragança, 5300-253 Bragança, Portugal

[3]CIMO – Mountain Research Center, Polytechnic Institute of Bragança, 5300-253 Bragança, Portugal

[4]Department of Chemistry, Indian Institute of Technology Madras, Chennai 600 036, India

*Corresponding author: Pedro J. Carvalho, E-mail address: quijorge@ua.pt

1 **ABSTRACT**

2   Due to the costs involved, the capture of CO_2 in post-combustion is not currently seen

3   as economically viable. Aiming at changing the perception of post-combustion CO_2 from a

4   costly and non-profitable process to a valuable commodity and fostering the development of

5   the next-generation of technologies, novel solvents and their mixtures have been investigated.

6   In this work, mixtures of non-volatile ionic liquids were screened by COSMO-RS aiming to find

7   mixtures with positive excess volumes that could present an increased CO_2 capture by physical

8   sorption. The most promising mixtures identified by COSMO-RS, $[C_4C_1im][DMP]$ or

9   $[C_4C_1im][NTf_2]$ + carboxylate-based protic ILs were characterized through the measurement of

10 their thermophysical properties, namely density and viscosity. Both properties were measured

11 for pure ILs and their binary mixtures at different temperatures and compositions. The

12 temperature dependence of density of pure ILs was described using the Gardas and Coutinho

13 model while viscosity was accurately described using the Vogel–Tammann–Fulcher equation.

14 The Redlich-Kister equation was used to predict the excess molar volumes and the non-ideality

15 of the mixtures' viscosity was assessed using the Grunberg and Nissan mixing law. The excess

16 molar volumes for mixtures containing $[C_4C_1im][DMP]$ show large positive values all over the

17 range of compositions and temperatures, making them good candidates for CO_2 capture. To the

18 best of our knowledge, the excess molar volumes obtained in this work were the highest

19 reported so far. COSMO-RS was able to correctly predict the trend of the experimental excess

20 molar volumes for these mixtures. Regarding viscosity, mixtures of $[C_4C_1im][DMP]$ with the

21 carboxylate-based protic ILs led to the desired viscosity decrease compared to the pure aprotic

22 IL, and large deviations from ideality were observed. The mixing of ILs is thus an efficient way to

23 fine-tune the properties, in this case decreasing the viscosity while increasing the sorption

24 capacity.

25

26 **Keywords:** ILs mixtures, COSMO-RS, Density, Excess molar volumes, Viscosity.

1 **1. Introduction**

2 Human dependency and consumption on fossil fuels is a major source of

3 greenhouse gases (GHGs). Among the anthropogenic GHGs, carbon dioxide (CO_2)

4 stands as one with the most important contribution with over 84% energy-related

5 emissions. Its growing atmospheric concentration results from the fossil fuel

6 combustion, particularly power plant emissions [1]. The global economic expansion

7 and the rising energy demand in developing countries anticipates an increase of these

8 emissions in the near future, leading to concerns over permanent climate changes and

9 to the need to implement of climate-related initiatives capable to mitigate the GHGs

10 effects.

11 Currently, the conventional technology used in industry is based on amine

12 absorption processes that while presenting advantages, like operation stability, high

13 capacity and good reactivity; are also costly and may be environmentally harmful [2].

14 There is thus a growing interest in developing innovative technologies for an efficient

15 and economic capture of CO_2 [3]. Technologies involving adsorption, membrane

16 separation or carbamation stand as promising alternatives for CO_2 capture [3–7].

17 Due to their outstanding properties, ionic liquids (ILs) have been studied as

18 alternatives to replace solvents commonly used in physical sorption of CO_2 [3,8,9].

19 Their tunability, low vapour pressure, thermal stability and high solvating capacity

20 [10,11] make this class of neoteric solvents suitable for CO_2 capture and separation

21 from other streams. However, most ILs present high viscosities limiting their industrial

22 application. The possibility of fine-tuning their properties through their structural

23 manipulation or formulated mixtures, may allow to overcome the current limitations

24 while keeping the solvation potential [9]. Although mixing ILs with different molecular

25 weights and chemical structures can be used to tune the solvent viscosity, it is also

26 known for the negative impact on the sorption capacity. The correct selection of ILs

27 may however overcome this limitation by tuning the Hildebrand solubility parameter,

28 matching the solubility parameter of the ILs mixture with that of the gas of interest,

29 or/and increase the solvent free volume and thus, increasing the gas solubility. In fact,

30 several studies have proposed mixtures of ILs with lower viscosities while enhancing

3

1 the CO_2 solubility and selectivity [12–14]. Nevertheless, the available data is scarce and

2 discrepancies are observed among the authors, which calls for further studies in this

3 field [8]. The first step is to provide a complete thermophysical characterization of ILs

4 mixtures that, albeit of indisputable importance, is still scarce. These data, combined

5 to CO_2 solubility measurements, will be of great interest for the development of

6 theoretical tools, like equations of state, correlations, group contribution models, and

7 more importantly for their implementation in process simulators to accurately design

8 and scale-up industrial separation processes.

9 Density and viscosity, the physical properties investigated in this work, are of great

10 importance in absorption processes. If on the one hand, an increased viscosity can

11 significantly reduce the mass transfer coefficients causing slower diffusion of CO_2 to

12 the bulk liquid and leading to larger separation unities [15]; on the other, systems with

13 positive excess volumes are expected to have enhanced physical solubility due to the

14 increase of the solvent free volume and thus, higher solubility.

15 The large number of possible ionic liquids mixtures to be investigated makes

16 impractical an exhaustive characterization of these systems. Thus, the use of

17 experimental data for the validation of computational tools, like the Conductor-like

18 Screening Model for Real Solvents – COSMO-RS – predictive model [16], is essential so

19 that models can be used for a screening and identification of the ionic liquids, and their

20 mixtures, with the highest potential for a given purpose.

21 Knowing that the solubility of gases in pure ionic liquids is ruled by physisorption

22 with the gas occupying the free volume within the ILs voids [8,17,18], COSMO-RS was

23 used here as a predictive tool to identify the most promising mixtures of ionic liquids

24 with positive deviations from ideality (i.e. activity coefficients, γ, greater than one) and

25 thus, expectably, positive excess volumes and consequently enhanced solubility.

26 However, it is important that this increased non-ideality does not promote a complete

27 phase separation, previously reported for specific ionic liquid mixtures [19–21].

28 However, for ionic liquid mixtures, Omar et al. [22] reported that mixtures presenting

29 excess enthalpies higher than 500 J·mol^{-1} usually lead to phase separation. Therefore,

1   in this work the selection of the mixtures was carried using these two constraints:

2   positive deviations from ideality and excess enthalpies lower than 500 J·mol^{-1}.

3   Aiming to establish grounds for the development of new and sustainable

4   technologies capable of meeting the global climate change goals and to expand the

5   state of carbon management options, the characterization of mixtures of ILs is here

6   carried out. COSMO-RS is used to make an extensive screening of the ionic liquids and

7   ionic liquids families with the highest potential for the proposed separation. Then the

8   thermophysical characterization of their densities and viscosities is addressed, allowing

9   to understand the behaviour/property duality necessary for the development of

10 theoretical models and to build a complete description of the solvent properties.

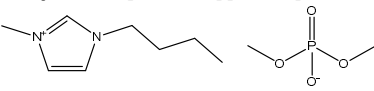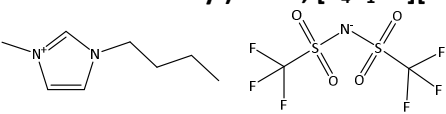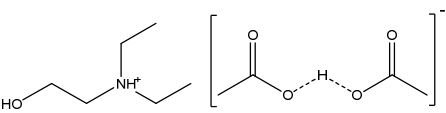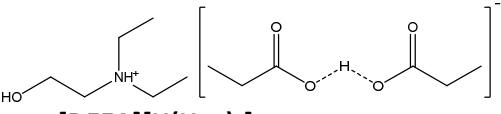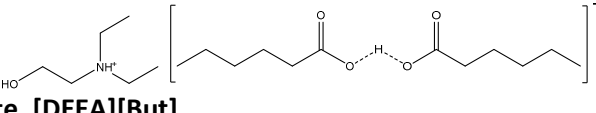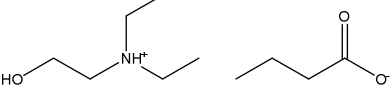11 **2. Experimental**

12 **2.1. Chemicals**

13 Six protic ionic liquids based on the *N,N*-diethylethanolammonium ([DEEA]$^+$) or *N*-

14 butyl-2-hydroxyethyl ammonium ([BHEA]$^+$) cations combined with the anions Acetate

15 ([Ace]$^-$), Propanoate ([Prop]$^-$), Butanoate ([But]$^-$), Pentanoate ([Pent]$^-$) or Hexanoate

16 ([Hex]$^-$) and the aprotics 1-butyl-3-methylimidazolium dimethylphosphate,

17 ([C$_4$C$_1$im][DMP]) or 1-butyl-3-methylimidazolium bis(trifluoromethanesulfonyl)imide

18 ([C$_4$C$_1$im][NTf$_2$]) were used in this work. The ionic liquids name, mass fraction purity,

19 molecular weight, supplier and chemical structure are reported in Table 1. The water

20 content of the ionic liquids and their mixtures was determined by a Metrohm 831 Karl

21 Fischer coulometer using the analyte Hydranal®—Coulomat AG from Riedel-de Haën.

22 *Protic Ionic Liquid Synthesis*

23 The synthesis of the carboxylate-based protic ILs has been detailed in previous

24 publications [23,24]. To reduce the water content and volatile impurities, the ILs were

25 dried and purified under vacuum (1 Pa) at room temperature for at least 48 h. The

26 structures of the obtained compounds were analyzed by ^{1}H and ^{13}C NMR – Figure S1 of

27 supporting information. As can be seen by the ^{1}H NMR spectra, while the protic ILs

28 [DEEA][But], [DEEA][Pent] and [BHEA][Ace] are in the 1:1 (cation:anion) proportion;

29 the remaining are in the 1:2 (cation:anion) proportion due to the formation of an

1 azeotrope during the distillation purification step. As reported by Ribeiro et al. [25],

2 mixtures of organic superbases with carboxylic acids lead to the formation of

3 azeotropic mixtures with an acid/base proportion different from the initially prepared

4 1:1. This happens due to the ability of carboxylic acids to form strong hydrogen bonds

5 with the protic ionic liquid ion pair leading to an azeotropic composition rich in acid. A

6 similar behavior was observed by Yoshizawa et al. [26] for α-picoline + trifluroacetic

7 acid where the boiling point reaches a maximum at 67% of acid, corresponding to the

8 formation of the highly stable $H(TFA)_2^-$ anion. The fact that this was observed only for

9 three, out of six, protic ionic liquids prepared seems to be related with the vapor

10 pressure of the components and the extension of the purification step. Nonetheless,

11 shorter purifications steps would, regardless, lead to cation:anion proportions that

12 converge to the 1:2 equilibrium ratio. The change of composition has a direct influence

13 in the properties and applications of the compound and thus was here considered.

14 **Table 1.** Name, chemical structure, molecular weight, mass fraction purity and supplier
15 of the investigated compounds.

Compound	Chemical structure
1-butyl-3-methylimidazolium dimethylphosphate, [C₄C₁im][DMP] (Mw = 264.26 g mol⁻¹; *wt%* > 98ᵃ) Acquired from Iolitec	
1-butyl-3-methylimidazolium bis(trifluoromethanesulfonyl)imide, [C₄C₁im][NTf₂] (Mw = 419.36 g mol⁻¹; *wt%* > 99ᵃ) Acquired from Iolitec	
***N,N*-diethylethanolammonium diacetate, [DEEA][H(Ace)₂]** (Mw = 237.30 g mol⁻¹; *wt%* > 95ᵇ) Synthesized	
***N,N*-diethylethanolammonium dipropanoate, [DEEA][H(Prop)₂]** (Mw = 265.35 g mol⁻¹; *wt%* > 90ᵇ) Synthesized	
***N,N*-diethylethanolammonium dihexanoate, [DEEA][H(Hex)₂]** (Mw = 349.51 g mol⁻¹; *wt%* > 96ᵇ) Synthesized	
***N,N*-diethylethanolammonium butanoate, [DEEA][But]** (Mw = 205.30 g mol⁻¹; *wt%* > 96ᵇ) Synthesized	
***N,N*-diethylethanolammonium pentanoate, [DEEA][Pent]**	

(*Mw* = 219.33 g mol^{-1}; *wt%* > 97[b])
Synthesized
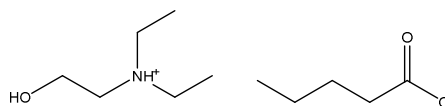
N-butyl-2-hydroxyethyl ammonium acetate, [BHEA][Ace]
(*Mw* = 177.24 g mol^{-1}; *wt%* > 96[b])
Synthesized

---
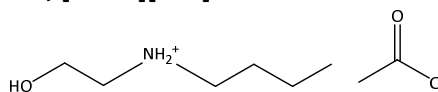
[a]Declared by the supplier; [b]Determined by NMR.

2.2. Methods

COSMO-RS

The Conductor-like Screening Model for Real Solvents is a predictive model for thermophysical properties of fluids and liquid mixtures based on unimolecular quantum calculations. Theoretical details can be found elsewhere [16,27]. Prior to the predictive process, TURBOMOLE 6.1 program package was used to generate the input files of the different molecules [28]. A BP functional B88-p86 with a triple-ξ valence polarized basis set (TZVP) and the resolution of identity standard (RI) approximation were used. ILs were described by an equimolar mixture of the lowest energy conformations of the cations and anions that contribute as two different compounds. COSMOtherm was then used to perform the statistical thermodynamics calculations using the BP_TZVP_C30_1701 (COSMOconfX v3.0, COSMOlogic GmbH & Co KG. Leverkusen, Germany) parameterization.

Mixtures preparation

Mixtures were prepared with the dried ILs in a dry-argon glove-box and at room temperature using an analytical balance model ALS 220-4N from Kern with a reproducibility of 0.2 mg. Vials with mixtures were heated at 323.15 K under stirring for at least 2h.

Density and viscosity

Densities and viscosities were measured using an automated SVM 3000 Anton Paar rotational Stabinger viscometer–densimeter (with a temperature uncertainty of 0.02 K, a dynamic viscosity relative uncertainty of 0.35% and a density absolute uncertainty of

5 x 10^{-4} g·cm^{-3}), working at atmospheric pressure. Densities and viscosities measurements were performed once for each sample but repeated with new random samples with similar compositions.

3. Results and Discussion

3.1. COSMO-RS screening

COSMO-RS was initially used to perform a screening of the ionic liquids mixtures with the highest potential for the CO_2 absorption. As starting point, the works of Claudio et al. [29], Omar et al. [22] and Moya et al. [30] were taken into account. Claudio et al. [29] used COSMO-RS to estimate the hydrogen-bond basicity of pure ILs and established polarity scales capable of ranking ILs according to their chemical behaviours, while Omar et al. [22] used the same tool to evaluate the mixing behaviour of IL–IL systems through the evaluation of the excess enthalpy. The non-ideal behaviour of mixtures of ionic liquids was analysed in-depth by Moya et al. [30].

Based on these studies, an initial set of compounds with the following criteria was chosen: ILs formed by the common [C_4C_1im] cation and the acetate, dimethylphosphate, bis(trifluoromethanesulfonyl)imide or hexafluorophosphate anions were chosen, due to the significant differences between their hydrogen-bonding interaction energies as stated in the work of Claudio et al. [29]; miscible mixtures with an excess enthalpy in the range [52 – 500] J·mol^{-1} were selected based on the article of Omar et al. [22]; and the two ILs mixtures with higher CO_2 solvation power identified by Moya et al. [30] ([C_2C_1im][DCN] + [C_2C_1im][NTf_2] and [C_2C_1im][NTf_2] + [C_2C_1im][$EtSO_4$]) were included. Fifteen carboxylate-based protic ILs investigated by us before [23,24,31] were also added to the screening pool, due to the reported potential CO_2 capture capacity [32,33].

More than 200 mixtures, composed by 9 cations and 12 anions (Table S1), were evaluated. The equimolar binary mixtures excess enthalpies (H^E) were calculated at 298.15 K using COSMO-RS – Table S2 and Figure S2 of Supporting Information. The ILs mixtures with activity coefficients greater than 1, that may lead to positive excess volumes and enhanced gas solubility, were selected for further characterization.

1 Furthermore, Omar et al. [22] reported that mixtures with excess enthalpies higher

2 than 500 J·mol^{-1} tend to be immiscible and thus, aiming to avoid phase separation, this

3 value was taken as an upper limit for the ILs mixtures selection as well.

4   Figure 1 depicts the IL-IL mixtures with positive excess enthalpies lower than 500

5 J·mol^{-1}, allowing one to identify mixtures composed of [C$_4$C$_1$im][DMP], [C$_4$C$_1$im][NTf$_2$]

6 or [C$_4$C$_1$im][PF$_6$] with the selected protic ILs, as those with the highest potential. In fact,

7 these mixtures present excess enthalpies two to three times higher than those

8 obtained for mixtures composed only by protic or aprotic ILs. Overall, mixtures of

9 [C$_4$C$_1$im][DMP] and [DEEA] cation-based ILs present the highest excess enthalpy values.

10 According with the work of Omar et al. [22] mixtures of ILs with similar ionic

11 constituents may lead to exothermic or an almost ideal mixing phenomena, i.e., excess

12 enthalpy close to zero, while IL – IL mixtures with significant structural differences lead

13 to systems with large deviations from ideality with endothermic mixing phenomena.

14   The selection was then narrowed down to seven systems (Figure 2), for further

15 physicochemical characterization. The systems [BHEA][Ace] + [C$_4$C$_1$im][DMP] and

16 [BHEA][Ace] + [C$_4$C$_1$im][NTf$_2$] were also included to explore the impact of changing the

17 protic cation and the aprotic anion.
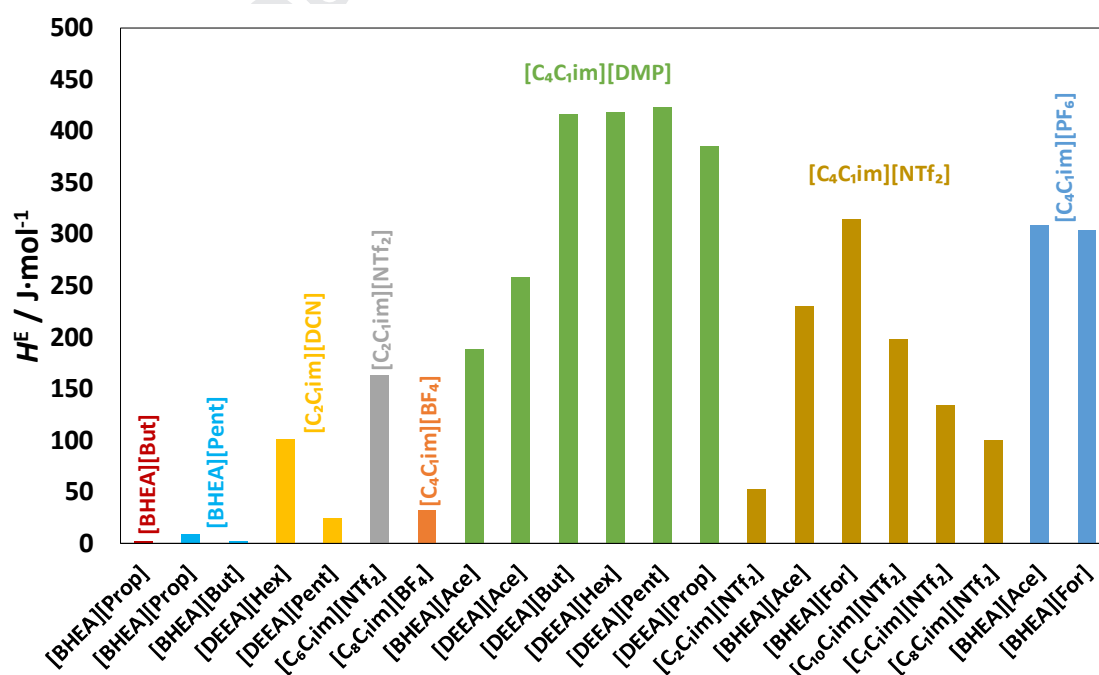
18

1   **Figure 1.** Binary equimolar mixtures with positive excess enthalpies, H^E, lower than 500

2   J·mol^{-1} at 298.15 K, computed by COSMO-RS.

3
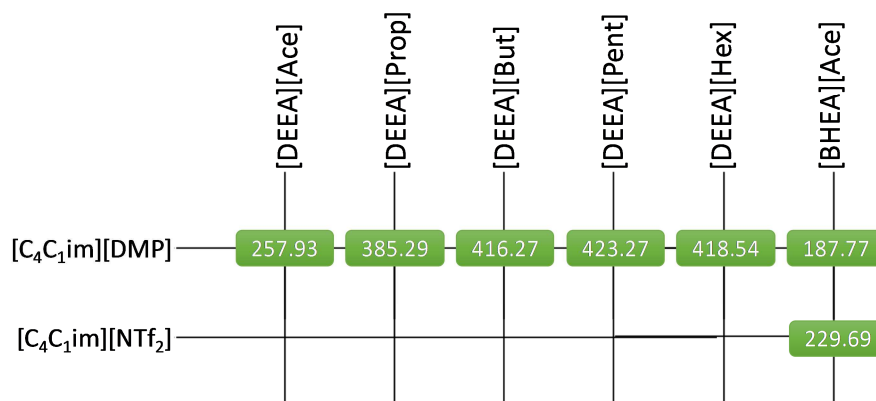
4   **Figure 2.** ILs mixtures selected and respective excess enthalpies (J·mol^{-1}) predicted by

5   COSMO-RS at 298.15 K and equimolar composition.

6

7   **3.2. Physicochemical properties**

8   *Density of the Pure Ionic Liquids*

9   Densities (ρ) of the pure ILs (water mass fractions lower than 1000 ppm) were

10 measured and are presented in Figure 3 and Table S3, along with the water content.

11 Increasing temperature leads to an increase in the molecular mobility and thus to a

12 decrease in the molecular packing and consequently in density. For each series, i.e.,

13 [DEEA][X] (X = But or Pent) and [DEEA][H(Y)$_2$] (Y = Ace, Prop or Hex), the increase of the

14 protic anion chain length leads to a decrease in the density, as observed before [34].

15 This property follows the decreasing order of the molecular weight of the anions

16 within the same series.
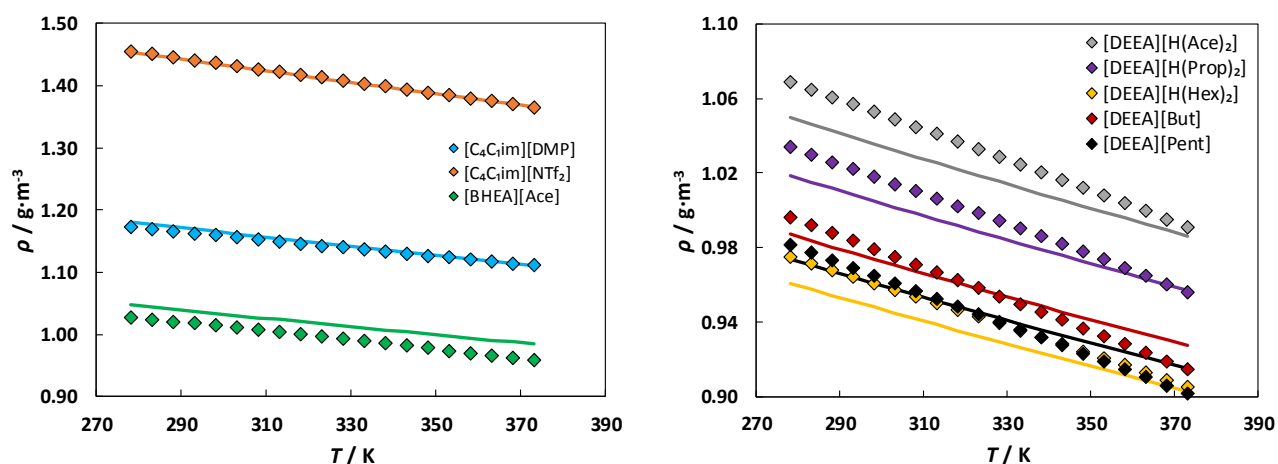
1 **Figure 3.** Density of the pure ILs as function of temperature and predictions (solid
2 lines) using Gardas and Coutinho [35] model.

3   Gong et al. [36], Almeida et al. [37] and Hiraga et al. [38] were some of the

4 authors reporting the density of $[C_4C_1im][DMP]$ at different temperatures. An average

5 relative deviation, $\%ARD = 1/N \sum_{i=1}^{N} |(X^{exp} - X^{lit})/X^{exp}|$ (where X represents the

6 property and the subscripts *exp* and *lit* the experimental and literature values,

7 respectively), between the experimental values and those reported in the literature of

8 0.2% was here observed. Regarding $[C_4C_1im][NTf_2]$, an *%ARD* of 0.1% was obtained in

9 relation with literature [37,39–41]. To the best of our knowledge the protic ILs

10 densities are here reported for the first time.

11   The Gardas and Coutinho model [35], an extension of the Ye and Shreeve group

12 contribution method [42], was used to describe the experimental density data:

13 $$\rho = \frac{Mw}{N \cdot V(a + b \cdot T + c \cdot p)}$$ (1)

14 where ρ is the density in $kg \cdot m^{-3}$, Mw is the molecular weight in $kg \cdot mol^{-1}$, N is the

15 Avogadro constant, and V is the volume in m^3. The volume is assumed as the linear

16 sum of the volumes of cation and anion [35]. a, b and c are coefficients previously

17 proposed: $a = 0.8005 \pm 0.0002$, $b = (6.652 \pm 0.007) \times 10^{-4}$ K^{-1} and $c = (-5.919 \pm 0.024) \times$

18 10^{-4} MPa^{-1} [35]. T and p are the absolute temperature in K and the pressure in MPa,

19 respectively. The cation and anion volumes were taken from literature: $[C_4C_1im]^+$ 238

20 $Å^3$ [35]; $[DMP]^-$ 139 $Å^3$ [43]; $[NTf_2]^-$ 248 $Å^3$ [35]; $[Ace]^-$ 83.5 $Å^3$ [34]; $[Prop]^-$ 112.5 $Å^3$ [34];

21 $[But]^-$ 141.5 $Å^3$ [34]; $[Pent]^-$ 170.5 $Å^3$ [34]; $[Hex]^-$ 199.5 $Å^3$ [34]. The volumes of

11

1 [H(Ace)$_2$]$^-$, [H(Prop)$_2$]$^-$ and [H(Hex)$_2$]$^-$ were estimated from the values of [Ace]$^-$, [Prop]$^-$,

2 [Hex]$^-$ and H (5 Å^3) [35]. The volumes of the cations [DEEA]$^+$ and [BHEA]$^+$, 209 and

3 201.5 Å^3, were obtained by adding the contribution of –CH$_2$– group, 28 Å^3, reported by

4 Ye and Shreeve [42] to the molecular volume of *N,N*-dimethylethanolammonium [34]

5 and *N*-methyl-2-hydroxyethylammonium [44] cations.

6 The percentage average relative deviations between the predicted densities,

7 using the above mentioned model, and the experimental data were: 0.26%,

8 [C$_4$C$_1$im][DMP]; 0.12%, [C$_4$C$_1$im][NTf$_2$]; 1.25%, [DEEA][H(Ace)$_2$]; 0.85%,

9 [DEEA][H(Prop)$_2$]; 0.99%, [DEEA][H(Hex)$_2$]; 0.60%, [DEEA][But]; 0.60%, [DEEA][Pent]

10 and 2.12%, [BHEA][Ace]. The model can correctly predict the densities of the aprotic

11 ILs in all the temperatures investigated. Regarding the protic ILs, significant differences

12 can be observed namely for compound containing small anions. Additionally, from

13 Figure 3 it can be seen that for all protic ILs the model predicts a different temperature

14 dependency compared to the experimental.

15 From the linear dependency of the density with temperature ($\ln \rho = A_0 + A_1 T$,

16 where A_0 and A_1 are fitting parameters and T is the absolute temperature), the isobaric

17 thermal expansion coefficient, α_p , can be calculated according to:

18 $$\alpha_p = -\frac{1}{\rho}\left(\frac{\partial \rho}{\partial T}\right)_p = -\left(\frac{\partial ln\rho}{\partial T}\right)_p = -A_1 \qquad (2)$$

19 In the temperature range investigated in this work, the use of a linear

20 regression to describe the experimental data is satisfactory, being the average relative

21 deviation between the experimental and calculated values of 0.04%.

22 Table 2 reports the thermal expansion coefficients at 0.1 MPa. For [DEEA]$^+$

23 based ILs, the thermal expansion coefficient decreases while increasing the molecular

24 weight of the protic IL, apart from [DEEA][H(Ace)$_2$] (Figure S3). Additionally, protic

25 [DEEA][X] ILs show greater values of α_p than the [DEEA][H(Y)$_2$]. These coefficients are a

26 measure of how the volume changes with temperature and thus, this behavior is

27 related to the packing of the hydrocarbon chains.

1 **Table 2.** Thermal expansion coefficients of the studied ionic liquids along with the
2 expanded uncertainty with an 95% level of confidence.

Ionic Liquid	$(10^4 \times \alpha_p \pm \sigma)$ / K^{-1}
[C$_4$C$_1$im][DMP]	5.72 ± 0.01
[C$_4$C$_1$im][NTf$_2$]	6.70 ± 0.01
[DEEA][H(Ace)$_2$]	7.91 ± 0.05
[DEEA][H(Prop)$_2$]	8.17 ± 0.07
[DEEA][H(Hex)$_2$]	7.82 ± 0.05
[DEEA][But]	8.97 ± 0.04
[DEEA][Pent]	8.90 ± 0.04
[BHEA][Ace]	7.32 ± 0.05

3 *Densities of the ILs mixtures*

4   The ILs mixtures densities, at different temperatures and compositions, are
5 presented in Tables S4 and depicted in Figure 4. As expected, the density of the
6 mixtures investigated decreases with increasing temperature and increases with the
7 increase of the molar fraction of [C$_4$C$_1$im][DMP] or [C$_4$C$_1$im][NTf$_2$], the denser
8 compounds in the mixtures. At 298.15 K and equimolar composition, the mixture
9 density decreases with the increase numbers of methyl groups in the protic IL anion in
10 each series (Figure 4-h). Regarding the anion, mixtures involving [C$_4$C$_1$im][NTf$_2$] are
11 denser than mixtures with [C$_4$C$_1$im][DMP]. The mentioned conclusions are in line with
12 the densities of the pure ionic liquids investigated.

13
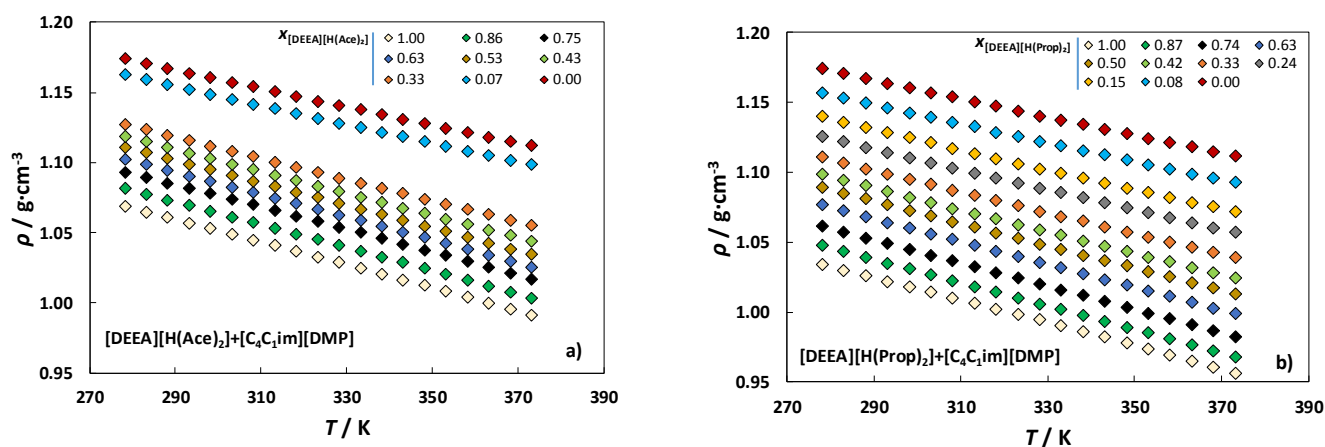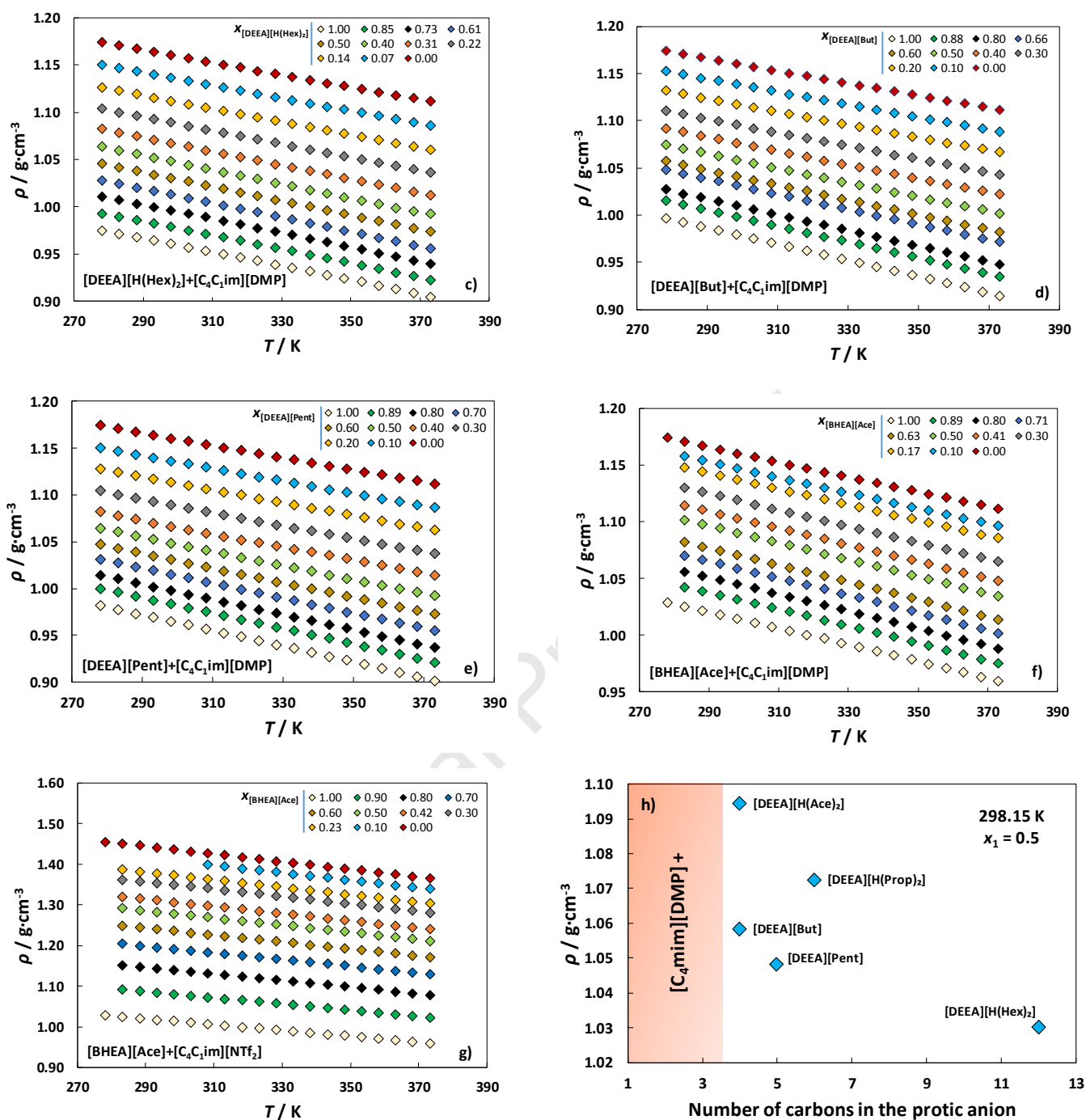
Figure 4. Densities of the investigated mixtures as a function of temperature and composition.

In order to better understand the nature of the molecular interactions in the binary mixtures, the excess molar volumes (V^E) were estimated according to the equation:

$$V^E = \frac{x_1 M_1 + x_2 M_2}{\rho_m} - \frac{x_1 M_1}{\rho_1} - \frac{x_2 M_2}{\rho_2} \qquad (3)$$

where x, M and ρ represent the mole fractions, molar masses and densities, respectively, of the mixture, m, or of the components (i = 1, 2).

Excess molar volumes result from physical and chemical interactions as well as structural contributions. While physical interactions involving weak dipole-dipole or dispersion forces increase the V^E, chemical interactions and structural contributions decrease the V^E [45]. In Figure 5 the excess molar volumes as function of the protic IL mole fraction (x_1) and temperature are depicted for the seven binary mixtures composed by the protic and aprotic ILs investigated.

The excess molar volumes were fitted to the Redlich-Kister [46] equation:

$$V_m^E = x_1(1 - x_1) \sum_{i=1}^{4}[A_i(T)(2x_1 - 1)^{i-1}] \tag{4}$$

with

$$A_i(T) = a_i + b_i(T/K) \tag{5}$$

and

$$\sigma = \left[\sum_{i=1}^{4} \frac{(V_{exp}^E - V_{calc}^E)_i^2}{n-k}\right]^{1/2} \tag{6}$$

where the values of the parameters (a_i and b_i) were determined using the method of least-squares, σ is the standard deviation, n is the number of experimental points and k is the number of coefficients. The parameters are summarized in Table S5 along with the standard deviations of the fit, and the predicted lines at 283.15, 323.15 and 373.15 K are plotted in Figure 5. Despite some discrepancies, the model is able to correctly describe the excess molar volumes at different temperatures and compositions.
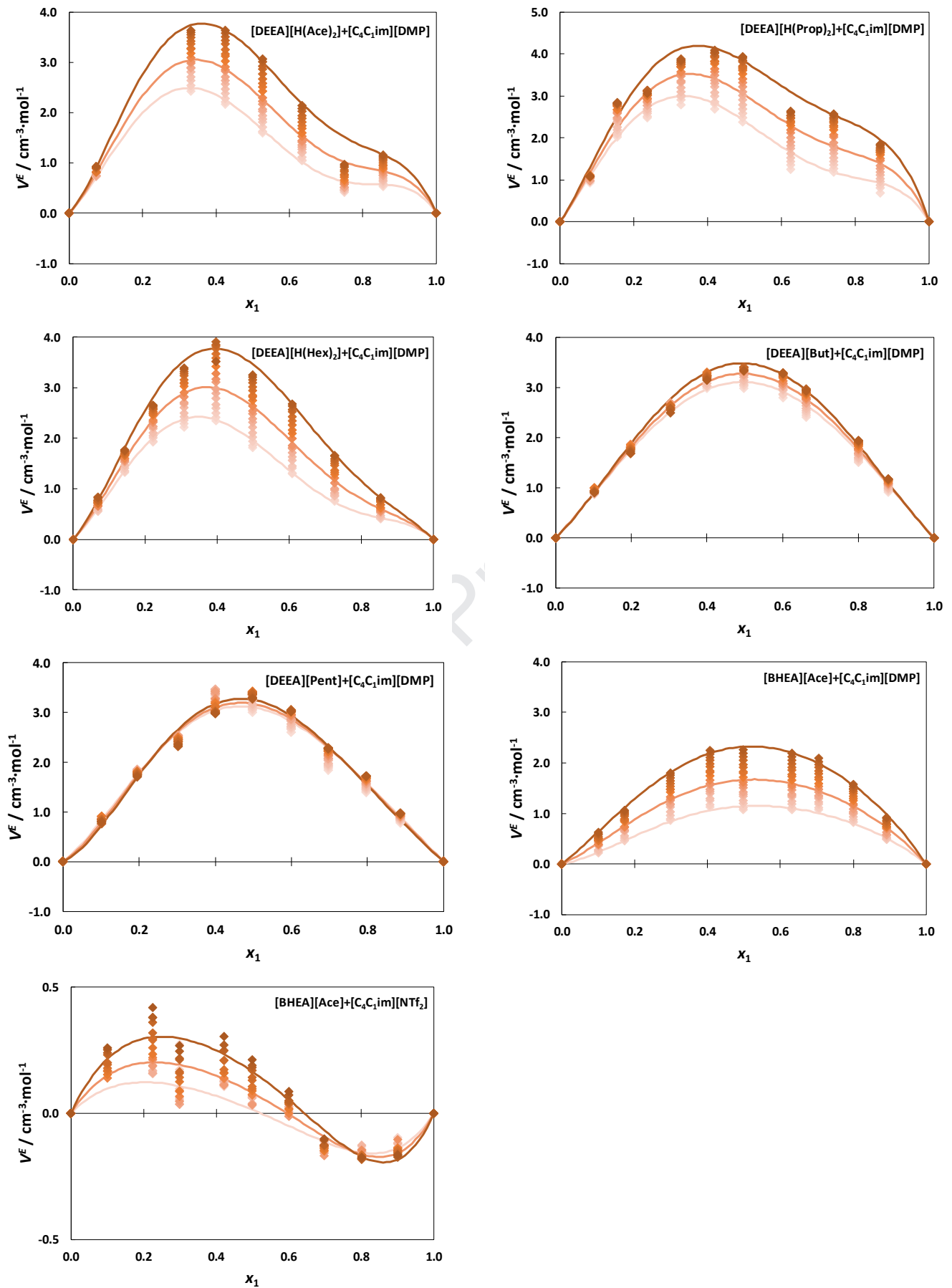
1 **Figure 5.** Excess molar volume versus mole fraction of IL (x_1 correspond to the protic IL)
2 for the binary systems investigated in this work at different temperatures. Light to dark
3 colours correspond to low to high temperatures (283.15 − 373.15) K. Solid lines
4 represent the Redlich−Kister equation at 283.15, 323.15 and 373.15 K.

5   The excess molar volumes of mixtures involving $[C_4C_1im][DMP]$ are positive
6 over the whole range of compositions and temperatures denoting less favorable
7 interactions between the species when compared to the pure compounds. Moreover,
8 this suggests more free space in these mixtures making them good candidates for CO_2
9 capture. The high values may be attributed to physical interactions that are not
10 compensated by the weak interactions between different molecules. When composed
11 by chemically distinct anions and cations, mixtures of ionic liquids have their first
12 solvation sphere disrupted by the different species increasing the possibility of larger
13 enthalpies of mixing [47]. The mixture involving $[C_4C_1im][NTf_2]$ shows an inversion in
14 the sign from positive to negative at $x_1 \geq 0.55$. This means that the interactions
15 between the ILs increase with the concentration of the protic IL.

16   The larger positive V^E values were observed for mixtures containing diacetate,
17 dipropanoate and dihexanoate indicating more free space between the molecules
18 when using $[DEEA][H(Y)_2]$ ILs. These three mixtures present asymmetrical V^E (x) curves
19 with a maximum around mole fractions of 0.33 of protic IL. Regarding the other
20 mixtures they all present symmetrical V^E (x) curves, with positive V^E. The increase of
21 temperature makes the excess molar volume more positive, indicating that the
22 mixture is more expansible than the pure compounds. Exceptions are
23 $[DEEA][But]+[C_4C_1im][DMP]$ $x_1 \leq 0.30$ and $[DEEA][Pent]+[C_4C_1im][DMP]$ $x_1 \leq 0.40$,
24 where the opposite behavior is observed.

25   When comparing the magnitude of the deviation from ideality observed
26 experimentally to that obtained from COSMO-RS predictions at 298.15 K and x_1=0.5
27 (Figure 1), for mixtures involving $[C_4C_1im][DMP]$ the model is able to correctly predict
28 that the V^E of $[DEEA][But]+[C_4C_1im][DMP]$ is approximately equal to that of
29 $[DEEA][Pent]+[C_4C_1im][DMP]$. Regarding $[BHEA][Ace] + [C_4C_1im][NTf_2]$ COSMO-RS fails,
30 predicting an excess enthalpy for this mixture higher than for $[BHEA][Ace] +$
31 $[C_4C_1im][DMP]$. Overall, this predictive tool is a valuable utensil for a preliminary quick

1   screen allowing to identify the ionic liquids families with the highest potential for CO_2

2   capture.

3   The positive excess molar volumes found in literature for IL mixtures are in

4   general small and very close to zero. The first extensive work on this was reported by

5   Rebelo et al. [48] that studied the volumes of mixing of mixtures of imidazolium-based

6   ILs containing $[NTf_2]^-$, $[BF_4]^-$ or $[PF_6]^-$ anions. All mixtures were found to have small

7   positive V^E, i.e., an almost linear mixing behaviour. In their review from 2012,

8   Niedermeyer et al. [49] cite several works on the subject and all are described as small

9   and positive (or negative). Thereafter, many works were published. Annat et al. [50]

10   for example measured the V^E of mixtures of $[C_3mpyr][NTf_2]$ and 5 other ILs obtaining

11   also small positive excess molar volumes in the order of [-0.3 to 1.8] $cm^3 \cdot mol^{-1}$. Clough

12   et al. [47] examined the physical properties of ten mixtures covering different types of

13   cations and anions, however, also here $V^E < 1.4$ $cm^3 \cdot mol^{-1}$ were achieved. More

14   recently, Brooks et al. [51] tried to establish the relationship between the structures,

15   free volumes and properties of ILs mixtures. They investigated several mixtures of ILs

16   and once more, excess molar volumes were found to be small and positive (or

17   negative). To the best of our knowledge, the excess molar volumes of the mixtures

18   investigated in this work are by far the highest reported to date promoting their use

19   and application.

20   *Viscosity of the Pure Ionic Liquids*

21   Due to their impact in mass transport phenomena, viscosity is a very important

22   property, in particular for CO_2 capture. Small viscosities increase the mass transfer

23   coefficients leading to a fast diffusion of CO_2 to the liquid bulk. The experimental

24   viscosity (η) of the pure ILs investigated (water mass fractions lower than 1000 ppm) as

25   function of temperature are listed in Table S3 and shown in Figure 6.

26   The ILs viscosity temperature dependency, generally depends on

27   intermolecular interactions like H-bonding and dispersive and Coulombic interactions

28   and these interactions decrease with increase temperature [52]. Thus, and as

29   expected, viscosity decreases with increasing temperature. For instance, for

1   [DEEA][H(Ace)$_2$] a rise in temperature from 278.15 to 373.15 K leads to a fall in

2   viscosity from 339.51 to 4.50 mPa·s. At 278.15 K, the viscosities follow the trend:

3   [BHEA][Ace] > [C$_4$C$_1$im][DMP] > [DEEA][H(Ace)$_2$] > [DEEA][H(Prop)$_2$] > [DEEA][But] >

4   [DEEA][H(Hex)$_2$] > [DEEA][Pent] > [C$_4$C$_1$im][NTf$_2$]; while at 373.15 K: [C$_4$C$_1$im][DMP] >

5   [BHEA][Ace] > [C$_4$C$_1$im][NTf$_2$] > [DEEA][H(Hex)$_2$] > [DEEA][H(Ace)$_2$] > [DEEA][H(Prop)$_2$] >

6   [DEEA][But] > [DEEA][Pent]. For the investigated compounds with a common cation

7   and within the same series ([DEEA][X] and [DEEA][H(Y)$_2$]), viscosity decreases with the

8   increase of the alkyl side chain length of the anion. At room temperature [DEEA]-based

9   ILs and [C$_4$C$_1$im][NTf$_2$] present small viscosities making them more interesting for

10   industrial applications.
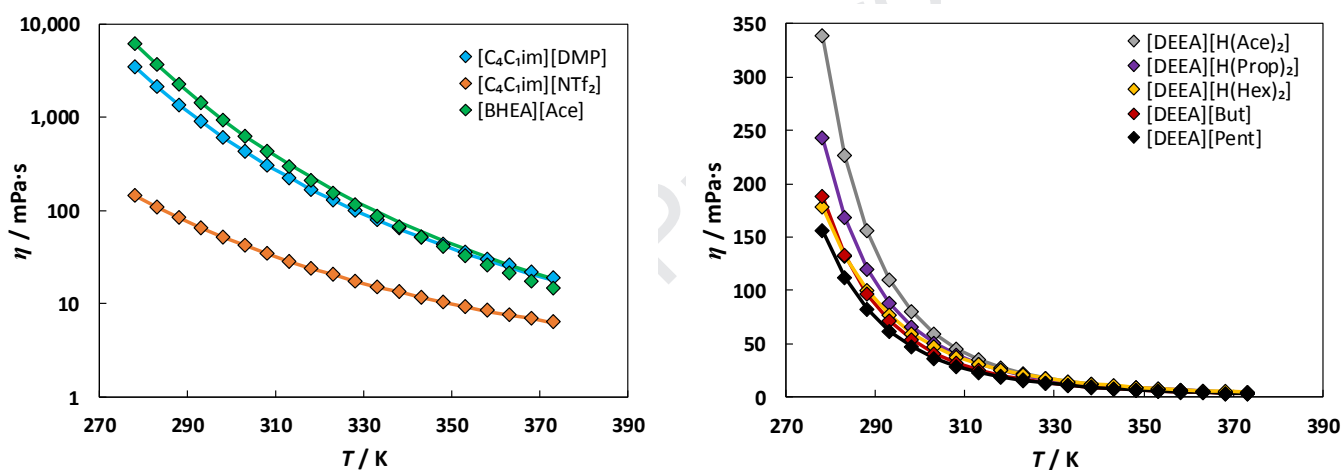
11   **Figure 6.** Viscosities of the pure ILs as function of temperature and calculated values
12   (solid lines) using the VTF equation.

13   Compared to density, in general larger deviations between sets of data by

14   different authors are observed for viscosity. The differences are usually due to the

15   well-known impact of water in this property [53]. Among others, Gong et al. [36] and

16   Hiraga et al. [38] reported the viscosity of [C$_4$C$_1$im][DMP] between 293 to 373 K. An

17   average relative deviation of 3.7 and 9.2%, respectively, to the data here published is

18   observed. While in this work [C$_4$C$_1$im][DMP] was dried and manipulated under a dry

19   atmosphere in order to avoid water absorption, Gong et al. [36] for example do no

20   mention any special care or the water content of the sample used in their

21   measurements. The experimental viscosity values for pure [C$_4$C$_1$im][NTf$_2$] measured in

1   this work are in good agreement with the values reported by Hiraga et al. [38] (%*ARD* =

2   1.3) and Liu et al. [41] (%*ARD* = 4.1).

3   The viscosities of pure ILs were fitted according the Vogel–Tammann–Fulcher

4   (VTF) model [53], expressed by equation (7). Based on the viscosity dependence with

5   the temperature, the energy barrier, *E*, was derived through equation (8).

6   $$\eta(T) = A_\eta exp\left[\frac{B_\eta}{T - C_\eta}\right] \qquad\qquad (7)$$

7   $$E = R\frac{\partial(ln[\eta(T)])}{\partial(1/T)} \qquad\qquad (8)$$

8   where A_η, B_η, and C_η are adjustable parameters (Table 3) estimated from

9   experimental data and *R* (J·K^{-1}·mol^{-1}) is the ideal gas constant.

10   Results show that the application of the VTF correlation provides a good

11 description of the viscosity dependence, as depicted in Figure 6 and Table 3. The only

12 exception is observed for [BHEA][Ace] with an %ARD of about 10%. This may be

13 explained by the enormous difference of the viscosity values at 278 and 373 K. The

14 differences in viscosity translate into different values of *E*; higher the viscosity, higher

15 the energy barrier of a fluid to shear stress and harder it is for the ions to move past

16 each other. At 298.15 K, [BHEA][Ace] is the ionic liquid with highest *E*, followed by

17 [C$_4$C$_1$im][DMP] while [C$_4$C$_1$im][NTf$_2$] presents the lowest value. Thus, [C$_4$C$_1$im][NTf$_2$] is

18 the IL that require less energy to move freely in the bulk, whereas [BHEA][Ace] and

19 [C$_4$C$_1$im][DMP] are those that need the more energy. This may be explained by the size

20 of the species, their symmetry and cation-anion interactions. Regarding the [DEEA]-

21 based cations, the energy barrier decreases while increasing the cation chain length

22 within the same series.

23 **Table 3.** Vogel–Tammann–Fulcher model parameters, %ARD and energy barrier *E* (at
24 298.15 K) of the studied ionic liquids together with the expanded uncertainty with an
25 95% level of confidence.

Ionic Liquid	($A_\eta \pm \sigma$) / mPa·s	($B_\eta \pm \sigma$) / K	($C_\eta \pm \sigma$) / K	%ARD / %	E / kJ·mol^{-1}
[C$_4$C$_1$im][DMP]	0.039 ± 0.002	1263.79 ± 13.96	167.47 ± 0.66	1.75	54.69 ± 1.41

[C$_4$C$_1$im][NTf$_2$]	0.149 ± 0.004	779.62 ± 6.95	164.95 ± 0.58	0.32	32.48 ± 0.70
[DEEA][H(Ace)$_2$]	0.024 ± 0.002	1072.73 ± 17.72	165.70 ± 1.03	1.38	45.19 ± 1.75
[DEEA][H(Prop)$_2$]	0.035 ± 0.001	1025.71 ± 3.24	162.36 ± 0.20	0.28	41.11 ± 0.30
[DEEA][H(Hex)$_2$]	0.021 ± 0.001	1317.17 ± 4.55	132.53 ± 0.28	0.21	35.49 ± 0.25
[DEEA][But]	0.014 ± 0.001	1247.94 ± 16.24	146.63 ± 0.95	0.75	40.17 ± 1.12
[DEEA][Pent]	0.015 ± 0.001	1253.33 ± 14.92	142.49 ± 0.90	0.60	38.23 ± 0.96
[BHEA][Ace]	0.014 ± 0.006	1518.39 ± 96.51	161.12 ± 4.00	10.39	59.76 ± 8.48

1   *Viscosities of the ILs mixtures*

2   The viscosity data for the selected binary mixtures of ILs are depicted in Figure

3   7 (versus temperature) and 8 (versus compositions) and listed in Table S6. Such as for

4   density, viscosity decrease with increasing temperature. Moreover, it increases with

5   the increasing concentration of the [C$_4$C$_1$im][DMP], excepting the [BHEA][Ace] +

6   [C$_4$C$_1$im][DMP] system where this only happens for temperatures higher than 338.15 K.

7   In [BHEA][Ace] + [C$_4$C$_1$im][NTf$_2$] viscosity decreases with the increase of the aprotic IL

8   due to their small viscosity when compared with the protic [BHEA][Ace]. Unlike

9   densities, viscosities do not vary linearly with the number of carbons in the protic

10   anion – Figure 7-h.
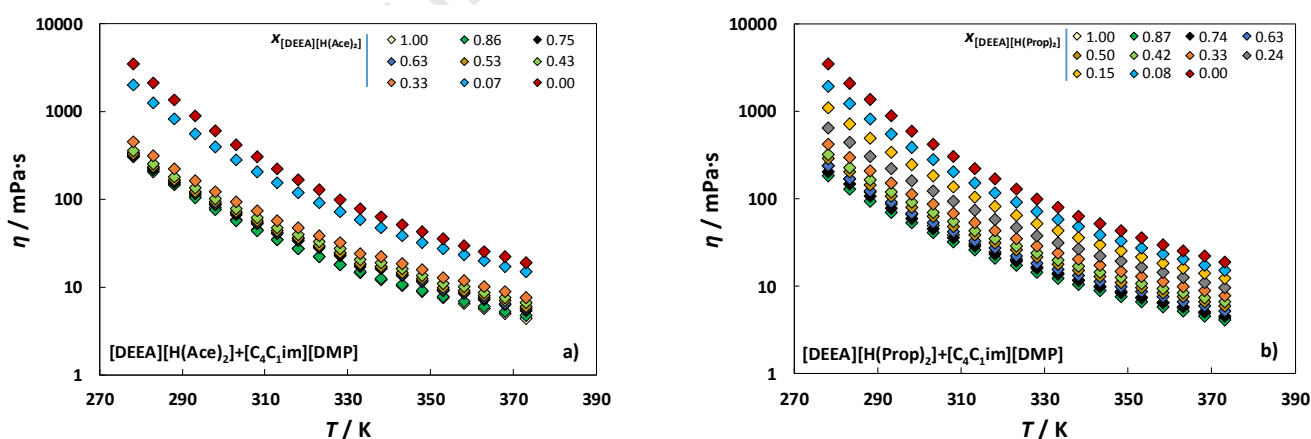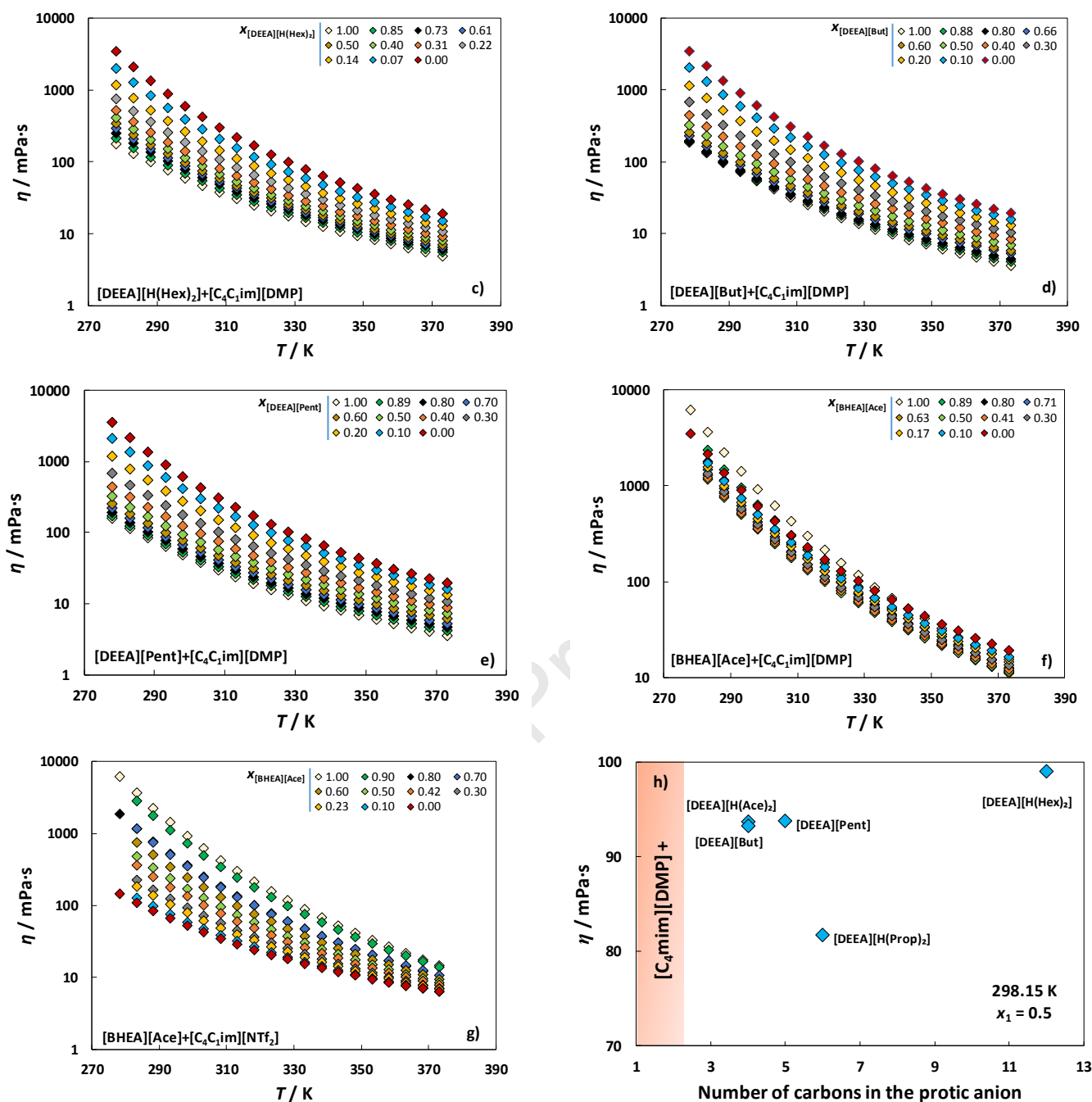
1 **Figure 7.** Viscosity of studied mixtures, and the correspondent pure ILs, as a function of
2 temperature and composition.

3 The non-ideality of the mixtures investigated was assessed using the Grunberg

4 and Nissan [54] mixing law where an additional parameter to account for non-ideality,

5 G_{12}, was included:

6 $$\ln \eta_m = x_1 \ln \eta_1 + x_2 \ln \eta_2 + x_1 x_2 G_{12}(T) \tag{9}$$

1   The optimum parameters determined for the studied mixtures are reported in

2   Table S7 and Figure 8 as function of temperature. As it can be seen in Figure 8, a good

3   description of the experimental data in all the composition ranges and temperatures

4   was obtained.

5
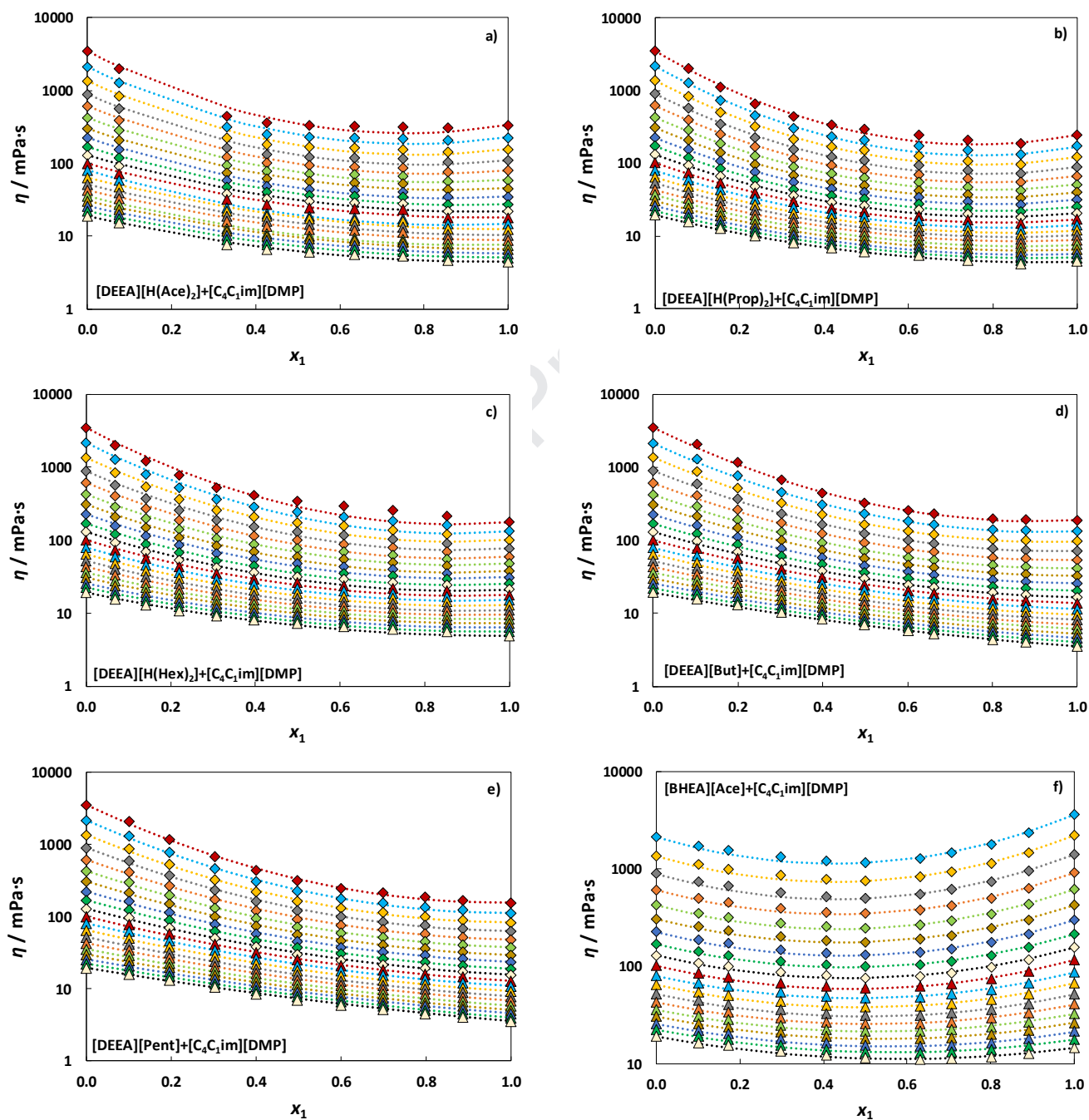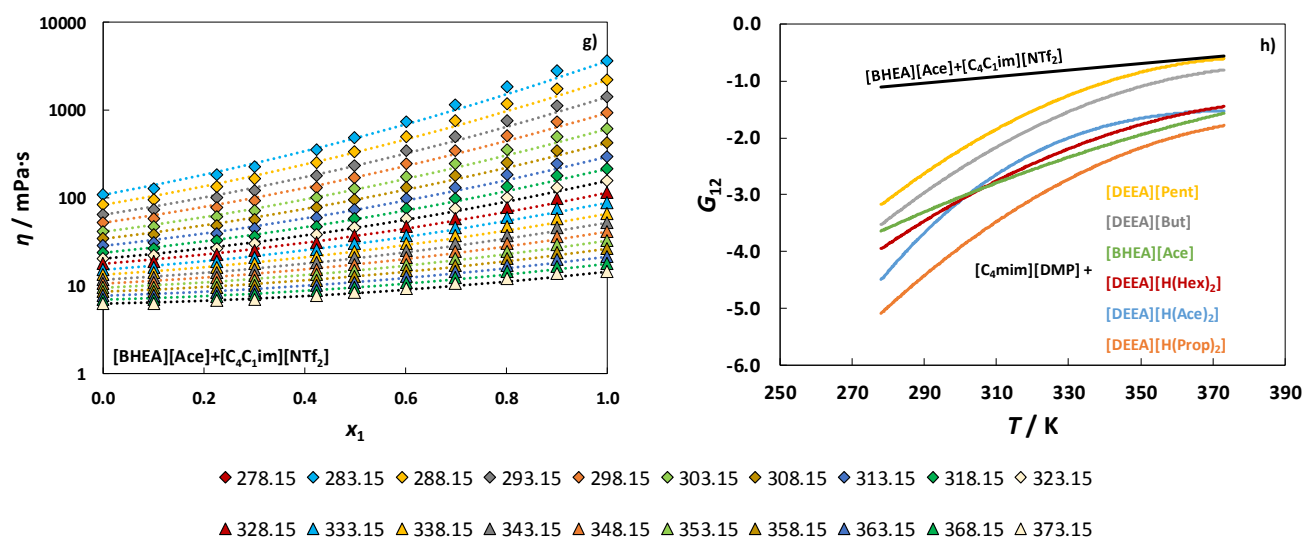
Figure 8. Viscosity versus mole fraction of the protic IL at different temperatures. Symbols represent experimental values and the solid curves represent the Grunberg and Nissan predictions.

The parameter G_{12} allows to quantify and express the deviations of the mixtures viscosity in relation to ideality (meaning $G_{12} = 0$) reported in Figure S4. Due to the chemical and size differences between the ILs, the systems investigated exhibit negative deviations from the ideal Grunberg and Nissan mixing law. Larger deviations are observed at low temperatures. [BHEA][Ace] + [C$_4$C$_1$im][NTf$_2$] are the mixtures closer to ideal behavior, especially at high temperatures, presenting a linear dependency of G_{12} with temperature – Figure 8-h. This is in agreement with the work of Almeida et al. [37] where the mixture of [C$_4$C$_1$im][Ace] + [C$_4$C$_1$im][NTf$_2$] that contains the same anions follows almost an ideal behavior.

4. Conclusions

This work contributes for the identification of promising mixture of ionic liquids to be used for the development of a cost-efficient CO_2 capture process. COSMO-RS was used to search for mixtures of ILs with positive excess enthalpies. Seven mixtures composed of [C$_4$C$_1$im][DMP] or [C$_4$C$_1$im][NTf$_2$], and carboxylate-based protic ILs, were selected and characterized by measuring their densities and viscosities at different temperatures and in the whole composition range. In general, large positive excess molar volumes and low viscosities were obtained for mixtures involving [C$_4$C$_1$im][DMP] making them good candidates for CO_2 capture. Thus, in this work it is shown the

1 possibility to fine-tune the properties of ILs by mixing them to achieve low viscosities

2 while keeping their sorption capacity.

15 **References**

16 [1] J.D. Figueroa, T. Fout, S. Plasynski, H. McIlvried, R.D. Srivastava, Advances in CO2

17   capture technology—The U.S. Department of Energy's Carbon Sequestration

18   Program, Int. J. Greenh. Gas Control. 2 (2008) 9–20. doi:10.1016/S1750-

19   5836(07)00094-1.

20 [2] B.A. Oyenekan, G.T. Rochelle, Energy Performance of Stripper Configurations for

21   CO 2 Capture by Aqueous Amines, Ind. Eng. Chem. Res. 45 (2006) 2457–2464.

22   doi:10.1021/ie050548k.

23 [3] M. Hasib-ur-Rahman, M. Siaj, F. Larachi, Ionic liquids for CO2 capture-

24   Development and progress, Chem. Eng. Process. Process Intensif. 49 (2010)

25   313–322. doi:10.1016/j.cep.2010.03.008.

26 [4] J. Gabrielsen, M.L. Michelsen, E.H. Stenby, G.M. Kontogeorgis, A Model for

27   Estimating CO 2 Solubility in Aqueous Alkanolamines, Ind. Eng. Chem. Res. 44

28   (2005) 3348–3354. doi:10.1021/ie048857i.

1   [5]   A.D. Ebner, J.A. Ritter, State-of-the-art Adsorption and Membrane Separation
2   Processes for Carbon Dioxide Production from Carbon Dioxide Emitting
3   Industries, Sep. Sci. Technol. 44 (2009) 1273–1421.
4   doi:10.1080/01496390902733314.

5   [6]   B.P. Mandal, M. Kundu, S.S. Bandyopadhyay, Physical solubility and diffusivity of
6   N2O and CO2 into aqueous solutions of (2-Amino-2-methyl-1-propanol +
7   monoethanolamine) and (N-methyldiethanolamine + Monoethanolamine), J.
8   Chem. Eng. Data. 50 (2005) 352–358. doi:10.1021/je049826x.

9   [7]   F. Barzagli, F. Mani, M. Peruzzini, A 13C NMR study of the carbon dioxide
10   absorption and desorption equilibria by aqueous 2-aminoethanol and N-methyl-
11   substituted 2-aminoethanol, Energy Environ. Sci. 2 (2009) 322–330.
12   doi:10.1039/b814670e.

13   [8]   P.J. Carvalho, K.A. Kurnia, J.A.P. Coutinho, Dispelling some myths about the CO_2
14   solubility in ionic liquids, Phys. Chem. Chem. Phys. 18 (2016) 14757–14771.
15   doi:10.1039/C6CP01896C.

16   [9]   C. Wu, T.P. Senftle, W.F. Schneider, First-principles-guided design of ionic liquids
17   for CO2 capture, Phys. Chem. Chem. Phys. 14 (2012) 13163–13170.
18   doi:10.1039/c2cp41769c.

19 [10] R.D. Rogers, CHEMISTRY: Ionic Liquids--Solvents of the Future?, Science. 302
20   (2003) 792–793. doi:10.1126/science.1090313.

21 [11] B. Kirchner, Ionic Liquids, Springer-Verlag Berlin Heidelberg, Heidelberg,
22   Germany, 2010.

23 [12] Z. Lei, J. Han, B. Zhang, Q. Li, J. Zhu, B. Chen, Solubility of CO_2 in Binary Mixtures
24   of Room-Temperature Ionic Liquids at High Pressures, J. Chem. Eng. Data. 57
25   (2012) 2153–2159. doi:10.1021/je300016q.

26 [13] H. Lin, B.D. Freeman, Materials selection guidelines for membranes that remove
27   CO2 from gas mixtures, J. Mol. Struct. 739 (2005) 57–74.
28   doi:10.1016/j.molstruc.2004.07.045.

29 [14] A. Finotello, J.E. Bara, S. Narayan, D. Camper, R.D. Noble, Ideal Gas Solubilities
30   and Solubility Selectivities in a Binary Mixture of Room-Temperature Ionic

Liquids, J. Phys. Chem. B. 112 (2008) 2335–2339. doi:10.1021/jp075572l.

[15] D. Song, A.F. Seibert, G.T. Rochelle, Mass Transfer Parameters for Packings: Effect of Viscosity, Ind. Eng. Chem. Res. 57 (2018) 718–729. doi:10.1021/acs.iecr.7b04396.

[16] A. Klamt, COSMO-RS From Quantum Chemistry to Fluid Phase Thermodynamics and Drug Design, Elsevier, Amsterdam, The Netherlands, 2005.

[17] L.Y. Wang, Y.L. Xu, Z.D. Li, Y.N. Wei, J.P. Wei, CO2/CH4 and H2S/CO2 Selectivity by Ionic Liquids in Natural Gas Sweetening, Energy and Fuels. 32 (2018) 10–23. doi:10.1021/acs.energyfuels.7b02852.

[18] G.R.M. Dowson, D.G. Reed, J.-M. Bellas, C. Charalambous, P. Styring, Fast and selective separation of carbon dioxide from dilute streams by pressure swing adsorption using solid ionic liquids, Faraday Discuss. 192 (2016) 511–527. doi:10.1039/C6FD00035E.

[19] A. Arce, M.J. Earle, S.P. Katdare, H. Rodríguez, K.R. Seddon, Application of mutually immiscible ionic liquids to the separation of aromatic and aliphatic hydrocarbons by liquid extraction: A preliminary approach, Phys. Chem. Chem. Phys. 10 (2008) 2538–2542. doi:10.1039/b718101a.

[20] G. Annat, M. Forsyth, D.R. MacFarlane, Ionic liquid mixtures-variations in physical properties and their origins in molecular structure, J. Phys. Chem. B. 116 (2012) 8251–8258. doi:10.1021/jp3012602.

[21] A. Arce, M.J. Earle, S.P. Katdare, H. Rodríguez, K.R. Seddon, Mutually immiscible ionic liquids, Chem. Commun. (2006) 2548–2550. doi:10.1039/B604595B.

[22] S. Omar, J. Lemus, E. Ruiz, V.R. Ferro, J. Ortega, J. Palomar, Ionic Liquid Mixtures—An Analysis of Their Mutual Miscibility, J. Phys. Chem. B. 118 (2014) 2442–2450. doi:10.1021/jp411527b.

[23] G. Sharma, D. Singh, S. Rajamani, R.L. Gardas, Influence of Alkyl Substituent on Optical Properties of Carboxylate-Based Protic Ionic Liquids, ChemistrySelect. 2 (2017) 10091–10096. doi:10.1002/slct.201701878.

[24] B.K. Chennuri, V. Losetty, R.L. Gardas, Apparent molar properties of

hydroxyethyl ammonium based ionic liquids with water and ethanol at various temperatures, J. Mol. Liq. 212 (2015) 444–450. doi:10.1016/j.molliq.2015.09.050.

[25] F.M.S. Ribeiro, C.F.R.A.C. Lima, A.M.S. Silva, L.M.N.B.F. Santos, Experimental Evidence for Azeotrope Formation from Protic Ionic Liquids, ChemPhysChem. 19 (2018) 2364–2369. doi:10.1002/cphc.201800335.

[26] M. Yoshizawa, W. Xu, C.A. Angell, Ionic Liquids by Proton Transfer: Vapor Pressure, Conductivity, and the Relevance of ΔpKa from Aqueous Solutions, J. Am. Chem. Soc. 125 (2003) 15411–15419. doi:10.1021/ja035783d.

[27] A. Klamt, F. Eckert, COSMO-RS: A Novel and Efficient Method for the A Priori Prediction of Thermophysical Data of Liquids, Fluid Phase Equilib. 172 (2000) 43–72. doi:http://dx.doi.org/10.1016/S0378-3812(00)00357-5.

[28] University of Karlsruhe and Forschungszentrum Karlsruhe GmbH, TURBOMOLE V6.1 2009, 1989–2007, 25 GmbH, since 2007; available from http://www.turbomole.com.

[29] A.F.M. Claudio, L. Swift, J.P. Hallett, T. Welton, J.A.P. Coutinho, M.G. Freire, Extended scale for the hydrogen-bond basicity of ionic liquids, Phys. Chem. Chem. Phys. 16 (2014) 6593–6601. doi:10.1039/C3CP55285C.

[30] C. Moya, M. Gonzalez-Miquel, F. Rodriguez, A. Soto, H. Rodriguez, J. Palomar, Non-ideal behavior of ionic liquid mixtures to enhance CO2 capture, Fluid Phase Equilib. 450 (2017) 175–183. doi:10.1016/j.fluid.2017.07.014.

[31] B.K. Chennuri, R.L. Gardas, Measurement and correlation for the thermophysical properties of hydroxyethyl ammonium based protic ionic liquids: Effect of temperature and alkyl chain length on anion, Fluid Phase Equilib. 427 (2016) 282–290. doi:10.1016/J.FLUID.2016.07.022.

[32] R. Vijayaraghavan, T. Oncsik, B. Mitschke, D.R. MacFarlane, Base-rich diamino protic ionic liquid mixtures for enhanced CO2 capture, Sep. Purif. Technol. 196 (2018) 27–31. doi:10.1016/J.SEPPUR.2017.06.057.

[33] X. Zhu, M. Song, Y. Xu, DBU-Based Protic Ionic Liquids for CO_2 Capture, ACS Sustain. Chem. Eng. 5 (2017) 8192–8198. doi:10.1021/acssuschemeng.7b01839.

[34] G. Sharma, R.L. Gardas, A. Coronas, G. Venkatarathnam, Effect of anion chain length on physicochemical properties of N,N-dimethylethanolammonium based protic ionic liquids, Fluid Phase Equilib. 415 (2016) 1–7. doi:10.1016/j.fluid.2016.01.036.

[35] R.L. Gardas, J.A.P. Coutinho, Extension of the Ye and Shreeve Group Contribution Method for Density Estimation of Ionic Liquids in a Wide Range of Temperatures and Pressures, Fluid Phase Equilib. 263 (2008) 26–32. doi:10.1016/j.fluid.2007.09.016.

[36] Y. Gong, C. Shen, Y. Lu, H. Meng, C. Li, Viscosity and Density Measurements for Six Binary Mixtures of Water (Methanol or Ethanol) with an Ionic Liquid ([BMIM][DMP] or [EMIM][DMP]) at Atmospheric Pressure in the Temperature Range of (293.15 to 333.15) K, J. Chem. Eng. Data. 57 (2011) 33–39. doi:10.1021/je200600p.

[37] H.F.D. Almeida, J.N. Canongia Lopes, L.P.N. Rebelo, J.A.P. Coutinho, M.G. Freire, I.M. Marrucho, Densities and Viscosities of Mixtures of Two Ionic Liquids Containing a Common Cation, J. Chem. Eng. Data. 61 (2016) 2828–2843. doi:10.1021/acs.jced.6b00178.

[38] Y. Hiraga, M. Goto, Y. Sato, R.L. Smith, Measurement of high pressure densities and atmospheric pressure viscosities of alkyl phosphate anion ionic liquids and correlation with the ε∗-modified Sanchez-Lacombe equation of state, J. Chem. Thermodyn. 104 (2017) 73–81. doi:10.1016/j.jct.2016.09.013.

[39] Y. Hiraga, A. Kato, Y. Sato, R.L. Smith, Densities at Pressures up to 200 MPa and Atmospheric Pressure Viscosities of Ionic Liquids 1-Ethyl-3-methylimidazolium Methylphosphate, 1-Ethyl-3-methylimidazolium Diethylphosphate, 1-Butyl-3-methylimidazolium Acetate, and 1-Butyl-3-methylimidazolium Bis(trifluoromethylsulfonyl)imide, J. Chem. Eng. Data. 60 (2015) 876–885. doi:10.1021/je5009679.

[40] C.A. Nieto de Castro, E. Langa, A.L. Morais, M.L.M. Lopes, M.J.V. Lourenço, F.J.V. Santos, M.S.C.S. Santos, J.N.C. Lopes, H.I.M. Veiga, M. Macatrão, J.M.S.S. Esperança, C.S. Marques, L.P.N. Rebelo, C.A.M. Afonso, Studies on the density,

heat capacity, surface tension and infinite dilution diffusion with the ionic liquids [C4mim][NTf2], [C4mim][dca], [C2mim][EtOSO3] and [Aliquat][dca], Fluid Phase Equilib. 294 (2010) 157–179. doi:10.1016/J.FLUID.2010.03.010.

[41] Q. Liu, L. Zhao, Q. Zheng, L. Mou, P. Zhang, Excess Molar Volume and Viscosity Deviation of [C_2mim][NTf_2]/[C_4mim][NTf_2] + DMC/DEC, J. Chem. Eng. Data. 63 (2018) 4484–4496. doi:10.1021/acs.jced.8b00591.

[42] C. Ye, J.M. Shreeve, Rapid and accurate estimation of densities of room-temperature ionic liquids and salts, J. Phys. Chem. A. 111 (2007) 1456–1461. doi:10.1021/jp066202k.

[43] M.G. Freire, A.R.R. Teles, M.A.A. Rocha, B. Schröder, C.M.S.S. Neves, P.J. Carvalho, D. V. Evtuguin, L.M.N.B.F. Santos, J.A.P. Coutinho, Thermophysical characterization of ionic liquids able to dissolve biomass, J. Chem. Eng. Data. 56 (2011) 4813–4822. doi:10.1021/je200790q.

[44] N.M.C.C. Talavera-Prieto, A.G.M.M. Ferreira, P.N. Simoes, P.J. Carvalho, S. Mattedi, J.A.P.J.A.P. Coutinho, P.N. Simões, P.J. Carvalho, S. Mattedi, J.A.P.J.A.P. Coutinho, Thermophysical characterization of N-methyl-2-hydroxyethylammonium carboxilate ionic liquids, J. Chem. Thermodyn. 68 (2014) 221–234. doi:10.1016/j.jct.2013.09.010.

[45] A.R. Mahajan, S.R. Mirgane, Excess Molar Volumes and Viscosities for the Binary Mixtures of n-Octane, n-Decane, n-Dodecane, and n-Tetradecane with Octan-2-ol at 298.15 K, J. Thermodyn. 2013 (2013) 1–11. doi:10.1155/2013/571918.

[46] O. Redlich, A.T. Kister, Algebraic Representation of Thermodynamic Properties and the Classification of Solutions, Ind. Eng. Chem. 40 (1948) 345–348. doi:10.1021/ie50458a036.

[47] M.T. Clough, C.R. Crick, J. Grasvik, P.A. Hunt, H. Niedermeyer, T. Welton, O.P. Whitaker, A physicochemical investigation of ionic liquid mixtures, Chem. Sci. 6 (2015) 1101–1114. doi:10.1039/C4SC02931C.

[48] J.N. Canongia Lopes, T.C. Cordeiro, J.M.S.S. Esperança, H.J.R. Guedes, S. Huq, L.P.N. Rebelo, K.R. Seddon, Deviations from ideality in mixtures of two ionic liquids containing a common ion, J. Phys. Chem. B. 109 (2005) 3519–3525.

1   doi:10.1021/jp0458699.

2   [49] H. Niedermeyer, J.P. Hallett, I.J. Villar-Garcia, P.A. Hunt, T. Welton, Mixtures of
3   ionic liquids, Chem. Soc. Rev. 41 (2012) 7780–7802. doi:10.1039/c2cs35177c.

4   [50] G. Annat, M. Forsyth, D.R. MacFarlane, Ionic Liquid Mixtures—Variations in
5   Physical Properties and Their Origins in Molecular Structure, J. Phys. Chem. B.
6   116 (2012) 8251–8258. doi:10.1021/jp3012602.

7   [51] N.J. Brooks, F. Castiglione, C.M. Doherty, A. Dolan, A.J. Hill, P.A. Hunt, R.P.
8   Matthews, M. Mauri, A. Mele, R. Simonutti, I.J. Villar-Garcia, C.C. Weber, T.
9   Welton, Linking the structures, free volumes, and properties of ionic liquid
10   mixtures, Chem. Sci. 8 (2017) 6359–6374. doi:10.1039/c7sc01407d.

11 [52] C.M.S.S. Neves, K.A. Kurnia, J.A.P. Coutinho, I.M. Marrucho, J.N.C. Lopes, M.G.
12   Freire, L.P.N. Rebelo, Systematic Study of the Thermophysical Properties of
13   Imidazolium-Based Ionic Liquids with Cyano-Functionalized Anions, J. Phys.
14   Chem. B. 177 (2013) 10271–10283. doi:10.1021/jp405913b.

15 [53] M.A.R. Martins, C.M.S.S. Neves, K.A. Kurnia, P.J. Carvalho, M.A.A. Rocha,
16   L.M.N.B.F. Santos, S.P. Pinho, M.G. Freire, Densities, viscosities and derived
17   thermophysical properties of water-saturated imidazolium-based ionic liquids,
18   Fluid Phase Equilib. 407 (2015) 188–196. doi:10.1016/j.fluid.2015.05.023.

19 [54] L. Grunberg, A.H. Nissan, Mixture law for viscosity, Nature. 164 (1949) 799–800.
20   doi:10.1038/164799b0.

21

Declaration of interests

☒ The authors declare that they have no known competing financial interests or personal relationships that could have appeared to influence the work reported in this paper.

☐The authors declare the following financial interests/personal relationships which may be considered as potential competing interests: